

Crystal-field analysis of the magnetic properties measured on a $\text{Ho}_2\text{Co}_{15}\text{Si}_2$ single crystal

Ming-hui Yu

Shenyang National Laboratory for Materials Science and International Centre for Materials Physics, Institute of Metal Research, Chinese Academy of Sciences, Shenyang 110016, People's Republic of China
and Van der Waals-Zeeman Instituut, Universiteit van Amsterdam, Valckenierstraat 65, 1018 XE Amsterdam, The Netherlands

Y. Janssen, O. Tegus, and J. C. P. Klaasse

Van der Waals-Zeeman Instituut, Universiteit van Amsterdam, Valckenierstraat 65, 1018 XE Amsterdam, The Netherlands

Zhi-dong Zhang

Shenyang National Laboratory for Materials Science and International Centre for Materials Physics, Institute of Metal Research, Chinese Academy of Sciences, Shenyang 110016, People's Republic of China

E. Brück, F. R. de Boer, and K. H. J. Buschow

Van der Waals-Zeeman Instituut, Universiteit van Amsterdam, Valckenierstraat 65, 1018 XE Amsterdam, The Netherlands

(Received 31 July 2001; revised manuscript received 27 March 2002; published 28 May 2002)

We have measured the magnetic properties of a $\text{Ho}_2\text{Co}_{15}\text{Si}_2$ single crystal in the temperature range 5–350 K with magnetic fields applied on the free crystal and along three major crystallographic directions of the fixed crystal. The temperature dependence of the magnetization measured on the free crystal shows that the Ho and Co moments compensate at 35 K, and continuous plane-cone-axis spin-reorientation transitions take place in a certain temperature range above room temperature. The field dependence of the total magnetization shows strong differences when measured along the three main crystallographic directions. In particular, this is the case at low temperatures where the magnetic isotherms are indicative of field-induced magnetic phase transitions. The magnetic isotherms at high temperatures show a marked magnetization anisotropy. We have analyzed our data, especially the field-induced and temperature-induced magnetic phase transitions in terms of a two-sublattice model in which the molecular-field interaction, the crystal-field interaction, and the moment anisotropy are important ingredients. A set of crystalline-electric-field parameters as well as the Ho-Co exchange field has been determined for the $\text{Ho}_2\text{Co}_{15}\text{Si}_2$ single crystal by fitting the experimental results with model calculations. The calculated magnetic behavior shows a good agreement with the experimental results in the temperature range presently studied, demonstrating the reliability of the determined parameters. It has been found that the Ho moment changes slightly in value during the spin-reorientation transition, and that there is a distinct magnetization anisotropy in the magnetic isotherms at high temperatures. These phenomena are intimately related to the marked direction dependence of the Ho moment.

DOI: 10.1103/PhysRevB.65.224409

PACS number(s): 75.10.Dg, 75.30.Gw, 75.50.Gg, 75.60.Ej

I. INTRODUCTION

The magnetic properties of rare-earth–transition-metal (R - T) intermetallics have attracted intensive studies, because of their great potential for application. Several interesting temperature-induced and field-induced phenomena, such as spin-reorientation transitions (SRT's), moment compensation, first-order moment reorientations, and moment bending sometimes occur in R - T compounds. Investigation of these phenomena usually reveals the intrinsic properties of the compounds, which is helpful for a better understanding of the magnetism of R - T systems. The change of the magnetic properties of $R_2\text{Co}_{17}$ -type compounds upon Si substitution has been an interesting topic in this field.^{1–3} Investigation of polycrystalline $\text{Ho}_2\text{Co}_{17-x}\text{Si}_x$ compounds has indicated that the compound with $x=2$ exhibits various interesting magnetic phenomena.² In order to obtain a clear understanding of these phenomena and of the influence of substitution of Si for Co, a detailed investigation of the magnetic properties of a $\text{Ho}_2\text{Co}_{15}\text{Si}_2$ single crystal would be of great significance.

In a previous investigation,⁴ a brief report on the magnetic properties of a $\text{Ho}_2\text{Co}_{15}\text{Si}_2$ single crystal was given. The easy magnetization direction (EMD) was found to be parallel to the c axis in an extended temperature region below the Curie temperature. According to the anomaly in the temperature dependence of magnetization measured in a low field, a discontinuous plane-axis SRT was thought to take place at 323 K with increasing temperature. Comparing these results with those obtained previously on various $R_2\text{Co}_{17}$ single crystals⁵ revealed that Si substitution leads not only to a sign reversal of the Co-sublattice anisotropy but also to a substantial anisotropy of the saturation magnetization. The sign and magnitude of the magnetization anisotropy were conserved during the spin-reorientation transition. A later investigation performed on a single crystal of $\text{Y}_2\text{Co}_{15}\text{Si}_2$ pointed out that only 32% of the anisotropy of the saturation magnetization in $\text{Ho}_2\text{Co}_{15}\text{Si}_2$ can be attributed to the Co sublattice.⁶ Preliminary crystal-field calculations made for the latter compound indicated that the strong directional dependence of the Ho moment in $\text{Ho}_2\text{Co}_{15}\text{Si}_2$ is the cause of the remaining large part of the magnetization anisotropy. The marked sensitivity

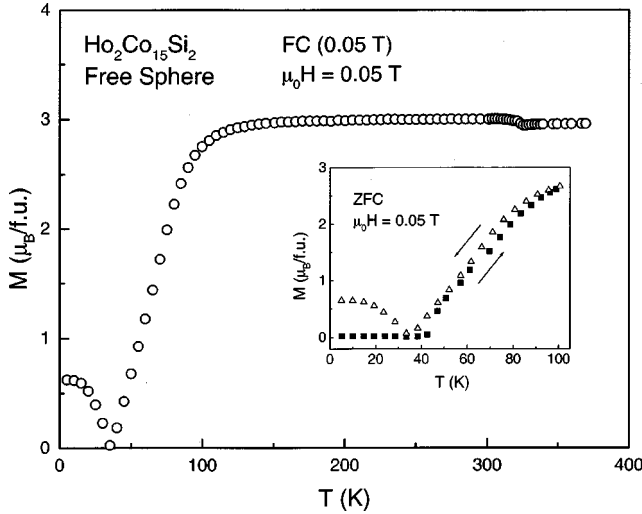


FIG. 1. Temperature dependence of the magnetic moment measured in a field of 0.05 T on a free sphere of a $\text{Ho}_2\text{Co}_{15}\text{Si}_2$ single crystal. The measurements were made with increasing temperature after the crystal was cooled to 5 K in the same field. The inset shows data obtained with increasing temperature without field cooling (filled squares) and data obtained with decreasing temperature (open triangles).

of the Ho moment to crystal-field effects led us to perform a more detailed crystal-field analysis of the magnetic properties of the $\text{Ho}_2\text{Co}_{15}\text{Si}_2$ single crystal. These crystal-field calculations together with some interesting experimental results will be presented in this paper.

The remainder of the present paper is organized as follows. The experimental procedure is described in Sec. II. Section III gives experimental results. In Sec. IV, we present the theoretical outline of the calculation method, and Sec. V gives calculation results of the crystal-field analysis. Section VI is for concluding remarks.

II. EXPERIMENT

A single-crystalline rod of $\text{Ho}_2\text{Co}_{15}\text{Si}_2$ was grown by means of a modified triarc Czochralski technique. The sample cut from this rod was shown by x-ray diffraction to have a rhombohedral $\text{Th}_2\text{Zn}_{17}$ structure. Electron probe microanalyzer examinations made on various parts of the single crystal confirmed the nominal composition.⁴

The magnetic measurements were made on a spherical sample of 2.9-mm diameter using a superconducting quantum interference device magnetometer in the temperature range 5–350 K. The anisotropic properties were studied in magnetic fields up to 5 T applied along various crystallographic directions. For measurements in higher fields, up to 9 T, we used an Oxford Instruments Maglab magnetometer.

III. EXPERIMENTAL RESULTS

A. Measurements on a free single crystal

The temperature dependence of the magnetic moment measured on the free single-crystalline $\text{Ho}_2\text{Co}_{15}\text{Si}_2$ sphere is shown in Fig. 1. The measurement was performed with in-

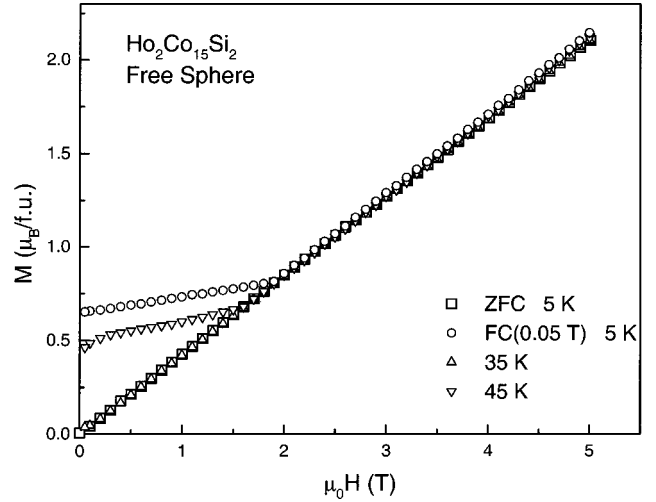


FIG. 2. Field dependence of the magnetic moment measured on a free sphere of a $\text{Ho}_2\text{Co}_{15}\text{Si}_2$ single crystal with decreasing field strength. The 5-K isotherms were obtained on a zero-field-cooled sample (open squares) and on a sample cooled to 5 K in a field of 0.05 T (open circles). The 35- and 45-K isotherms were obtained on zero-field-cooled samples.

creasing temperature after the crystal had been cooled to 5 K in the presence of a magnetic field of 0.05 T. In the temperature region below 100 K, the M - T curve reflects the feature of antiparallel coupling between the Co- and Ho-sublattice moments. A compensation temperature is evident at $T_{\text{comp}} = 35$ K. The compensation point was not observed in the previous investigation,⁴ where the single crystal was cooled to 5 K in zero field and the measurement was made with increasing temperature. As shown in the inset of Fig. 1, also in the present measurement there is no compensation temperature under such circumstances, but it is observed when the measurement is performed with decreasing temperature. The reason for this is the development of a multidomain structure in the sample when cooling in zero field. This multidomain structure leads essentially to zero net magnetization when the measuring field is much smaller than the coercive field. Cooling the crystal in an external field can retain the single-domain structure that is easily formed at high temperatures at low temperatures, which is important for experimentally observing the compensation point.

The presence of a multidomain structure at low temperatures is also manifest from the magnetic isotherms shown in Fig. 2. These isotherms were measured with decreasing field strength. By minimizing the free-energy expression, it can be shown that the low-temperature magnetization curve of a free single crystal comprises three regions.⁷ Below the critical field strength $B_{1,\text{crit}} = n_{\text{HoCo}} |M_{\text{Ho}} - M_{\text{Co}}|$, there is a strictly antiparallel alignment of the Ho moments and the Co moments: $M = |M_{\text{Ho}} - M_{\text{Co}}|$. At sufficiently high values of the applied field, $B > B_{2,\text{crit}}$, the Ho and Co moments are parallel: $M = M_{\text{Ho}} + M_{\text{Co}}$. The latter situation is not reached in the present experiments. In the intermediate field range, $B_{1,\text{crit}} < B < B_{2,\text{crit}}$, there exists a canted-moment configuration where the Ho- and Co-sublattice moments increasingly bend toward each other with increasing B . In this region, the field

dependence of the total moment is given by $M = B/n_{\text{HoCo}}$. From the slope of the M - B curve in this intermediate linear regime, one can therefore straightforwardly determine the experimental value of the molecular-field coefficient n_{HoCo} from which then the intersublattice coupling-constant J_{HoCo} can be obtained. This linear intermediate regime is reached at all three temperatures considered in Fig. 2. From the slope, which is practically the same at all three temperatures, showing that the intersublattice-coupling constant does not depend much on temperature, one obtains $n_{\text{HoCo}} = 2.33 \text{ T f.u.}/\mu_B$ (f.u. means a formula unit) and $J_{\text{HoCo}} = -7.0 \text{ K}$. Concentrating on the three field-cooled (FC) isotherms, the curve obtained at $T_{\text{comp}} = 35 \text{ K}$ passes through the origin because $B_{1,\text{crit}} = n_{\text{HoCo}}|M_{\text{Ho}} - M_{\text{Co}}|$ is zero at the compensation temperature. On both sides of T_{comp} the net magnetic moment increases and consequently the critical fields are nonzero in these cases. In contrast with this expected behavior, it is found that the 5-K isotherm measured after the zero-field cooling does not show a break marking the critical field but passes through zero. This behavior is attributed to the presence of a multidomain structure and strong magnetic anisotropy in the basal plane at 5 K. The strong in-plane anisotropy forces the Ho and Co moments to bend along the c direction, not in the plane. Because the EMD is in the basal plane, the domain walls are parallel to the c direction. The bending along the c direction makes the field parallel to the domain walls, i.e., the c direction. Therefore, the multidomain structure in the crystal can be retained, even if the field is increased to 5 T. In this case, the magnetization measured in fields above $B_{1,\text{crit}}$ should be the same as that in the case of a single-domain structure obtained by field cooling the crystal. However, when the field is below $B_{1,\text{crit}}$ the magnetization will decrease to zero if the field decreases to zero in the case of a multidomain structure, while it will keep the value of $M = |M_{\text{Ho}} - M_{\text{Co}}|$ in the case of a single-domain structure. The slight slope of the 5-K FC isotherm below $B_{1,\text{crit}}$ is due to the field dependence of the Ho moment. As to the isotherms at 35 and 45 K, the magnetization curves do not depend on the cooling process. This means that the crystal is magnetically soft above the compensation temperature so that the external field can easily realize a single-domain structure in the crystal.

Returning to Fig. 1, it is interesting to note that a small discontinuity in the thermal magnetization curve exists at 323 K. At high temperature, the easy-axis anisotropy of the Co sublattice dominates the easy-plane anisotropy of the Ho sublattice.¹⁻³ Therefore, one deduces that the small discontinuity in the thermal magnetization curve may imply a discontinuous plane to axis SRT at 323 K in $\text{Ho}_2\text{Co}_{15}\text{Si}_2$.⁴ However, it is worth mentioning that the flat thermal behavior of the moment above 100 K suggests that a measuring field of 0.05 T is not sufficient to form a single-domain structure in the crystal at high temperature. The reason for this is that the increase of the net moment causes a demagnetizing field higher than the measuring field of 0.05 T at high temperature. In order to avoid the influence of the demagnetizing field and to determine the real thermal behavior of the net moment at high temperature, the thermal curve was also measured in a field of 1 T (see Fig. 3), which is much larger

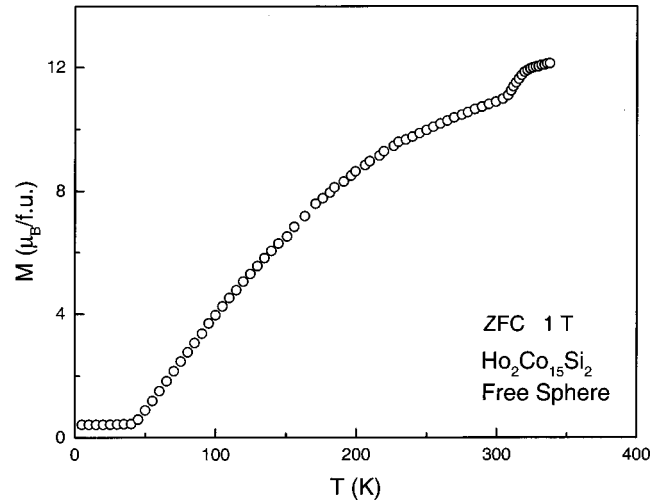


FIG. 3. Temperature dependence of the magnetic moment measured in a field of 1 T on a free sphere of a $\text{Ho}_2\text{Co}_{15}\text{Si}_2$ single crystal. The measurements were made with increasing temperature after the crystal was cooled to 5 K in zero field.

than the demagnetizing field. In this case, the anomalous thermal behavior of the net moment in the temperature range from about 305 to 320 K indicates that the SRT from easy plane to easy axis is not of first order but proceeds by a small intermediate easy-cone range. A detailed crystal-field analysis tells us that the anomalous thermal behavior of the net moment in the spin-reorientation temperature range comes from a marked direction dependence of both the Ho- and Co-sublattice moments, as will be discussed in detail later.

B. Measurements in different crystallographic directions

Magnetic isotherms measured in the three main crystallographic directions in the temperature range 100–350 K are displayed in Fig. 4. The isotherms in the two top panels confirm the change of EMD from the basal plane to the c axis with increasing temperature from 300 to 350 K. The magnetization anisotropy is distinct, that is, the saturation moment along the c axis is always larger than that in the basal plane direction, irrespective of the occurrence of a SRT. The results in the four lower panels in Fig. 4 show that magnetic hardness of the basal plane direction strongly increases with decreasing temperature. The results in the two lowest panels also show that magnetic anisotropy develops within the basal plane with decreasing temperature.

In order to further investigate the development of anisotropy within the basal plane, we have measured complete hysteresis loops at various temperatures below 100 K. These measurements were made with the field applied along the $[100]$ (a) direction as well as along the $[210]$ (b) direction. Results are shown in Figs. 5(a)–5(e). It is worth noting that the crystal is magnetically soft above the compensation temperature, and becomes hard below this temperature. This explains why the magnetization curve of the free single crystal at 5 K strongly depends on the cooling process. A point of considerable interest is the occurrence of jumplike changes in the isotherms. At 5 and 20 K, these changes are restricted

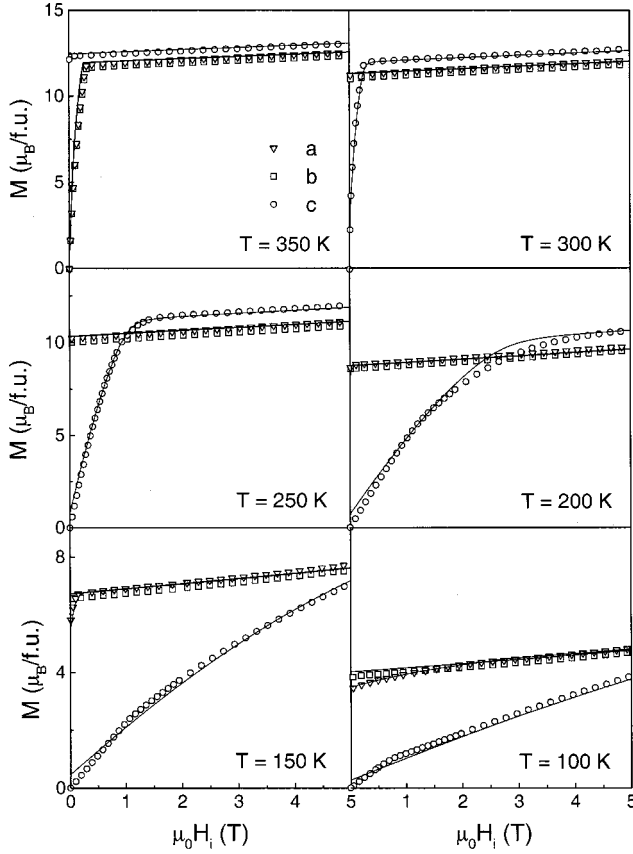


FIG. 4. Field dependence of the magnetic moment of a $\text{Ho}_2\text{Co}_{15}\text{Si}_2$ single crystal, measured with decreasing field at various temperatures in the three main crystallographic directions. There is a deviation of 4° from the c direction. The full curves through the data points are the result of crystal-field calculations.

to the a direction. At 65 K, it is only the b isotherm that gives rise to a jumplike change. Both the a and b isotherms display such a change at 50 K. However, no change can be observed in the a or b isotherms at 35 K. In order to be able to offer a reasonable explanation for the complex experimental data, the crystal-field theory in combination with a two-sublattice molecular-field model were employed to perform the theoretical analysis.

IV. THEORETICAL OUTLINE

$\text{Ho}_2\text{Co}_{15}\text{Si}_2$ has a $\text{Th}_2\text{Zn}_{17}$ -type rhombohedral structure with space group $R\bar{3}m$. In the coordinate system with the z and x axes along the c and a axes, respectively, the single-ion crystal-field Hamiltonian H_{CF} experienced by the Ho ion takes the form⁸

$$H_{\text{CF}} = \sum_n \sum_m B_n^m O_n^m = B_2^0 O_2^0 + B_4^0 O_4^0 + B_6^0 O_6^0 + B_6^6 O_6^6, \quad (1)$$

where $B_n^m = \theta_m \langle r^m \rangle A_n^m$, and where θ_m represents the Stevens coefficients (α_J , β_J , and γ_J for $m=2, 4$, and 6 , respectively), $\langle r^m \rangle$ are the Hartree-Fock radial integrals, and A_n^m are the crystalline-electric-field (CEF) parameters.

The total Hamiltonian of the Ho ion consists of three main contributions: the electrostatic CEF interaction, the Ho-Co exchange interaction, and the Zeeman energy, that is,

$$H_R = H_{\text{CF}} + 2(g_J - 1)\mathbf{J} \cdot \mathbf{B}_{\text{ex}} + g_J \mathbf{J} \cdot \mathbf{B}, \quad (2)$$

where \mathbf{J} is the total angular momentum of the Ho ion. The Ho-Ho exchange interaction, which is much weaker than the Ho-Co exchange interaction, is neglected. The exchange field $\mathbf{B}_{\text{ex}}(\mathbf{T})$ is assumed to be proportional and antiparallel to the magnetic moment of the Co sublattice $\mathbf{M}_{\text{Co}}(\mathbf{T})$, so one easily obtains

$$\begin{aligned} \mathbf{J} \cdot \mathbf{B}_{\text{ex}} = & -B_{\text{ex}}(J_x \sin \theta_{\text{Co}} \cos \phi_{\text{Co}} + J_y \sin \theta_{\text{Co}} \sin \phi_{\text{Co}} \\ & + J_z \cos \theta_{\text{Co}}), \end{aligned} \quad (3)$$

θ_{Co} and ϕ_{Co} are the polar and azimuthal angles of the Co moment with respect to the c axis and the a axis, respectively. As observed in $\text{Y}_2\text{Co}_{15}\text{Si}_2$,⁶ we have to consider the non-negligible anisotropy in the modulus of the Co moment, which can be expressed in manner^{9,10}

$$M_{\text{Co}}(T, \theta_{\text{Co}}) = M_{\text{Co}}(T)(1 - p \sin^2 \theta_{\text{Co}}), \quad (4)$$

where $p = 0.01$.⁶ The third term in the total Hamiltonian can be written as

$$\mathbf{J} \cdot \mathbf{B} = B(J_x \sin \theta_B \cos \phi_B + J_y \sin \theta_B \sin \phi_B + J_z \cos \theta_B), \quad (5)$$

where θ_B and ϕ_B are the polar and azimuthal angles of the external field with respect to the c and a axes, respectively.

For a given applied field \mathbf{B} and a direction of \mathbf{B}_{ex} , the eigenvalues E_i and the eigenfunctions $|i\rangle$ are obtained by diagonalizing the $(2J+1) \times (2J+1)$ matrix of the total Hamiltonian in the $|J, m\rangle$ representation:¹¹

$$\langle LSJm' | H_R | LSJm \rangle - E_i \delta_{m', m} = 0,$$

$$m, m' = -J, -J+1, \dots, J-1, J, \quad (6)$$

$$H_R |i\rangle = E_i |i\rangle, \quad i = 1, 2, \dots, 2J+1, \quad (7)$$

$$|i\rangle = \sum_{m=-J}^J a_m^i |J, m\rangle, \quad \sum_{m=-J}^J |a_m^i|^2 = 1. \quad (8)$$

The free energy of the $\text{Ho}_2\text{Co}_{15}\text{Si}_2$ is given by

$$F = -2k_B T \ln Z + K_{1\text{Co}} \sin^2 \theta_{\text{Co}} + K_{2\text{Co}} \sin^4 \theta_{\text{Co}} - \mathbf{M}_{\text{Co}} \cdot \mathbf{B}, \quad (9)$$

$$Z = \sum_{i=1}^{2J+1} \exp[-E_i/k_B T], \quad (10)$$

where Z is the partition function of the Ho ion, and $K_{1\text{Co}}$ and $K_{2\text{Co}}$ are the anisotropy constants of the Co sublattice. $K_{1\text{Co}}(T/T_c)$ and $K_{2\text{Co}}(T/T_c)$ are taken the same as for

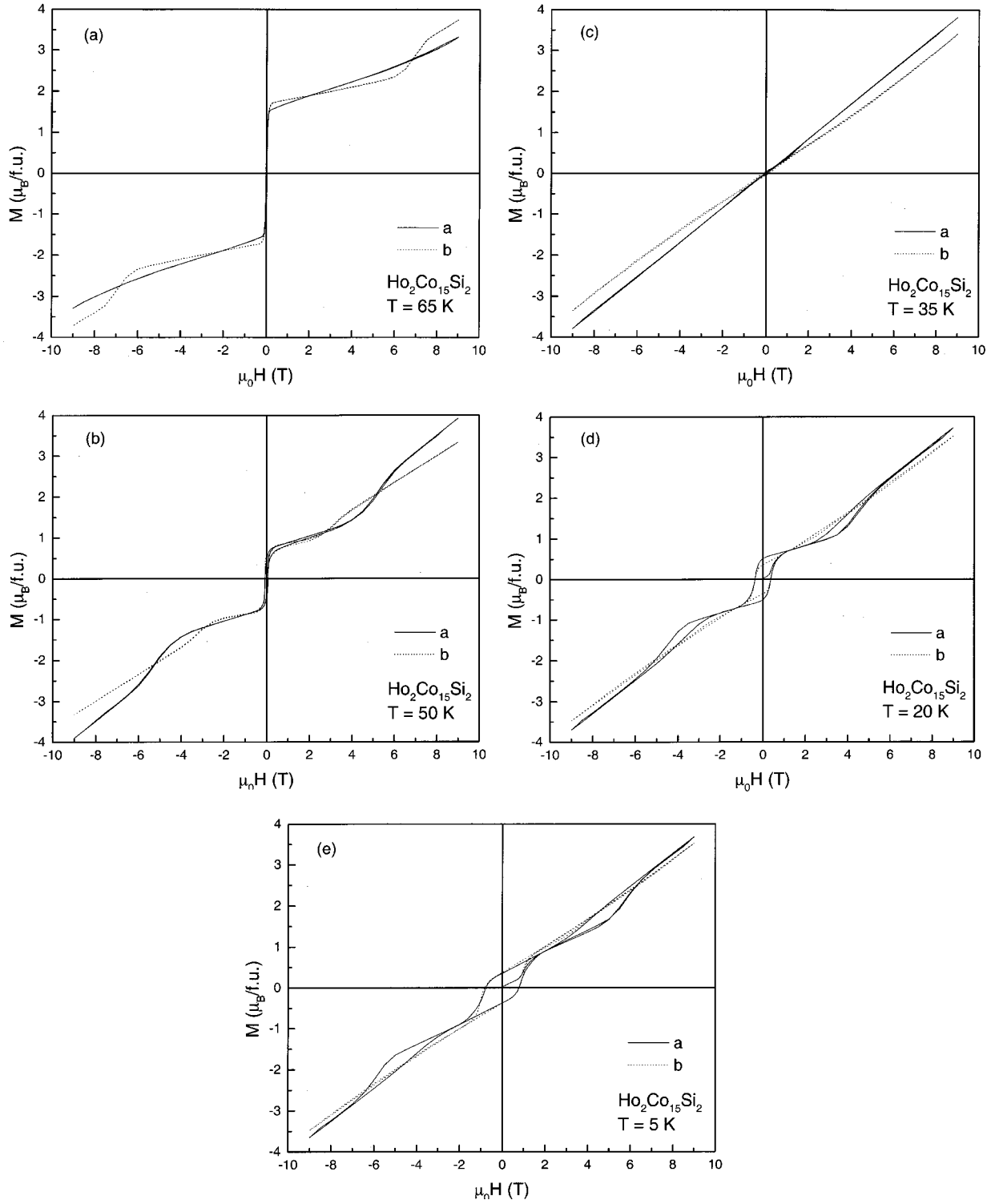


FIG. 5. Hysteresis loops of a $\text{Ho}_2\text{Co}_{15}\text{Si}_2$ single crystal measured in the a and b directions in a temperature range between 65 and 5 K.

$\text{Y}_2\text{Co}_{15}\text{Si}_2$.⁶ The equilibrium direction of \mathbf{B}_{ex} is determined from a minimization of the free energy. The magnetic moment of the Ho ion is thus given by

$$M_\gamma = - \sum_{i=1}^{2J+1} (i|J_\gamma|i) g_J \exp[-E_i/k_B T] / Z, \quad \gamma = x, y, z. \quad (11)$$

The total magnetic moment of the compound $\text{Ho}_2\text{Co}_{15}\text{Si}_2$ along the field direction is given by¹¹

$$M(B) = 2(M_x \sin \theta_B \cos \phi_B + M_y \sin \theta_B \sin \phi_B + M_z \cos \theta_B) + M_{\text{Co}} [\sin \theta_{\text{Co}} \sin \theta_B \cos(\phi_{\text{Co}} - \phi_B) + \cos \theta_{\text{Co}} \cos \theta_B]. \quad (12)$$

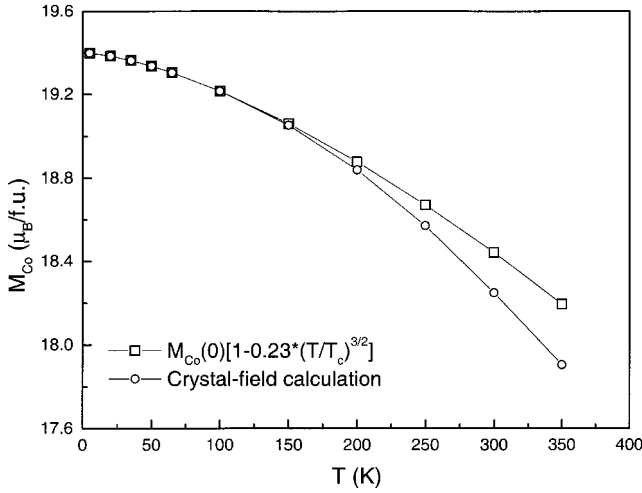


FIG. 6. Temperature dependence of the Co-sublattice moment measured for $\text{Y}_2\text{Co}_{15}\text{Si}_2$ (open squares), and the temperature dependence of the Co-sublattice moment per formula unit in $\text{Ho}_2\text{Co}_{15}\text{Si}_2$ as derived from the crystal-field calculation (open circles).

V. CRYSTAL-FIELD ANALYSIS

In this section, we shall use the well-established theoretical two-sublattice crystal-field model⁸⁻¹¹ described above to interpret the unusual magnetic phenomena observed experimentally. In the crystal-field fitting process, the Co moment, the exchange field and the crystal-field parameters were taken as adjustable quantities. All the data analyzed by the crystal-field theory have been corrected for demagnetization effects, H_i is the internal field and the demagnetization factor is considered to be $\frac{1}{3}$ for the sphere crystal. As input crystal-field parameters we used the values reported for $\text{Ho}_2\text{Co}_{17}$ by Han *et al.*⁸ ($A_2^0 = -134.3\text{Ka}_0^{-2}$, $A_4^0 = -13.6\text{Ka}_0^{-4}$, $A_6^0 = 0.58\text{Ka}_0^{-6}$, and $A_6^6 = -19.4\text{Ka}_0^{-6}$). The final values of the parameters that led to the optimum fit with our experimental data are $M_{\text{Co}}(0) = 19.4\mu_B/\text{f.u.}$, $B_{\text{ex}}(0) = 76.0\text{ K}$, A_2^0

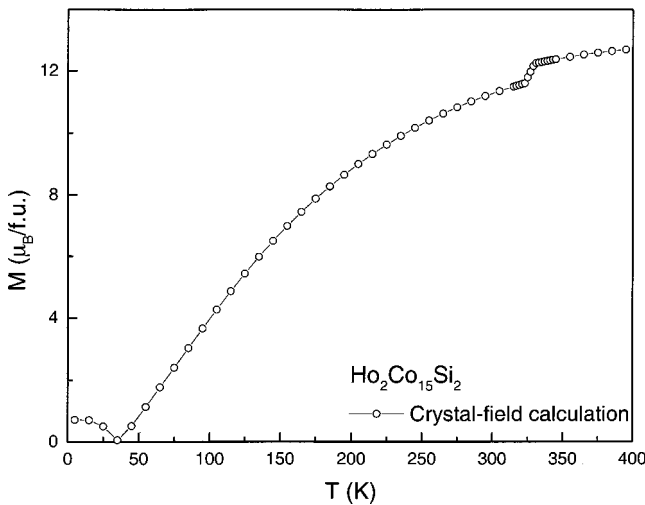


FIG. 7. Temperature dependence of the spontaneous total magnetic moment of $\text{Ho}_2\text{Co}_{15}\text{Si}_2$ as derived from the crystal-field calculation.

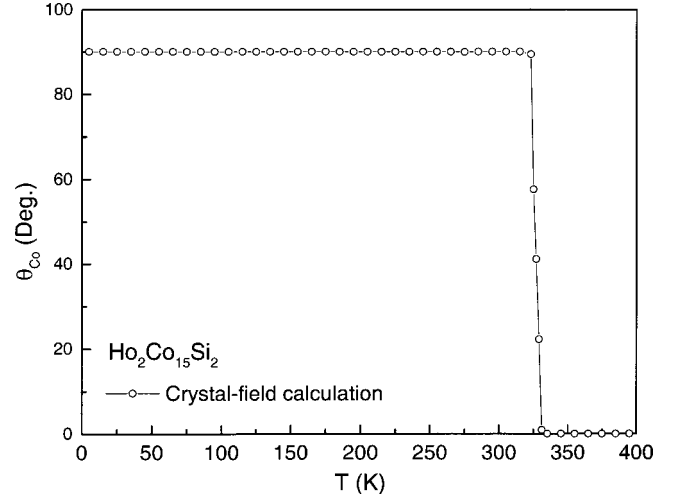


FIG. 8. Temperature dependence of the Co-sublattice moment direction relative to the c direction in $\text{Ho}_2\text{Co}_{15}\text{Si}_2$ as derived from the crystal-field calculation.

$= -182.0\text{Ka}_0^{-2}$, $A_4^0 = 5.0\text{Ka}_0^{-4}$, $A_6^0 = 0.6\text{Ka}_0^{-6}$, and $A_6^6 = -20.0\text{Ka}_0^{-6}$. The substitution of Si for Co changes many parameters used in the theoretical model, such as the crystal-field parameters, the Co moment, the Co moment anisotropy, the Ho-Co exchange field and so on. In Fig. 6, the results of the crystal-field fit show that the Co-sublattice moment in $\text{Ho}_2\text{Co}_{15}\text{Si}_2$ decreases a little faster than that in $\text{Y}_2\text{Co}_{15}\text{Si}_2$ with increasing temperature. This may come from a slight decrease of Co-Co exchange interaction due to the substitution of Ho for Y in $R_2\text{Co}_{17}$ -type compounds. That is why the Curie temperatures 1195 K of $\text{Ho}_2\text{Co}_{17}$ and 837 K of $\text{Ho}_2\text{Co}_{15}\text{Si}_2$ are almost the same as those 1192 K of Y_2Co_{17} and 836 K of $\text{Y}_2\text{Co}_{15}\text{Si}_2^1$, respectively, even if the substitution of Ho for Y brings about Ho-Co exchange interaction. The substitution of Si for Co decreases the Curie temperature rapidly at an approximate rate of 178 and 179 K per Si atom for the $\text{Ho}_2\text{Co}_{17-x}\text{Si}_x$ and $\text{Y}_2\text{Co}_{17-x}\text{Si}_x$ compounds, respectively.^{1,2} The effect of magnetic dilution and the de-

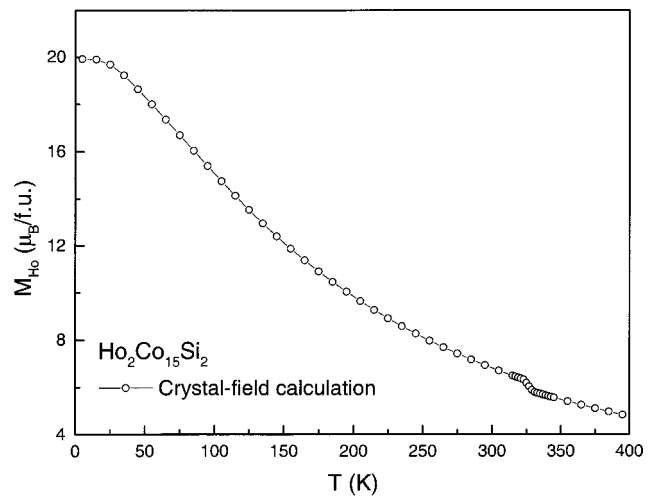


FIG. 9. Temperature dependence of the Ho-sublattice moment in $\text{Ho}_2\text{Co}_{15}\text{Si}_2$ as derived from the crystal-field calculation.

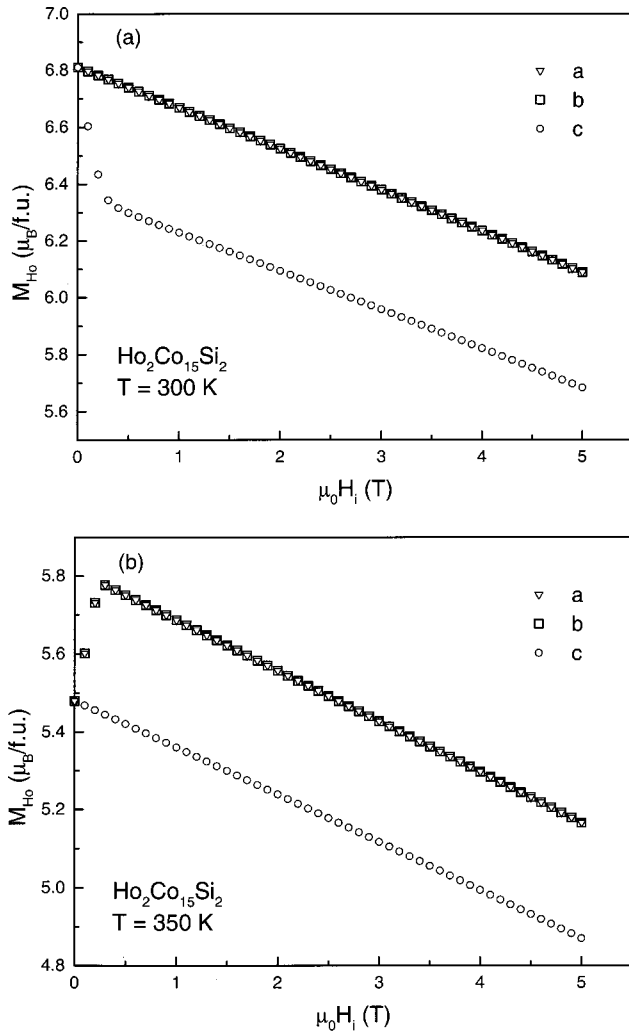


FIG. 10. Field dependence of the Ho-sublattice moment in $\text{Ho}_2\text{Co}_{15}\text{Si}_2$ at (a) 300 K and (b) 350 K as derived from crystal-field calculations for magnetic fields applied along the three major crystallographic directions.

crease of the Co-Co exchange interaction and the Co moment per atom result in the rapid decrease of T_c with increasing Si concentration. It is worth noting that the substitution of Ho for Y in $R_2\text{Co}_{15}\text{Si}_2$ does not change the Co moment at absolute zero temperature. The same case has also been found in $R_2\text{Co}_{17}$ compounds.⁸ In comparison with $1.7\mu_B$ per atom in metallic Co, the formation of $R_2\text{Co}_{17}$ slightly decreases the Co moment to $1.63\mu_B$ per atom, and the discrepancy of influence from different rare earths is negligible.⁸ However, the substitution of Si for Co leads to a marked decrease of Co moment to $1.29\mu_B$ per atom in $R_2\text{Co}_{15}\text{Si}_2$ at a rate of $0.17\mu_B$ per Si atom. It is well known that the large spatial extent of $3d$ wave functions leads to the $3d$ -electron energy band rather than to the $3d$ level. Therefore, the change of the $3d$ -band structure by the substitution of Si and a transfer of the outer electrons of Si to the $3d$ band are responsible for the evident effect of Si on magnetic moment per Co atom. The detailed discussion was given in Ref. 6 about the fitting to the Bloch's law for the temperature dependence of Co moment in $\text{Y}_2\text{Co}_{15}\text{Si}_2$. The full line in

Fig. 6 is a fit to the data using the expression $M_S(T) = M_S(0)[1 - b(T/T_c)^n]$, with $b = 0.23$ and $n = 3/2$.⁶ This is in good agreement with the $T^{3/2}$ law of a very low temperature spin-wave approximation as discussed quantitatively by Dyson.¹²

According to the optimum crystal-field fit, the calculated temperature dependence of the total moment M of $\text{Ho}_2\text{Co}_{15}\text{Si}_2$ is shown in Fig. 7. These data compare well with the experimental results of the low-temperature part in Fig. 1 and the high-temperature part in Fig. 3. The Ho- and Co-sublattice moments theoretically compensate at 35 K, which agrees very well with the experimental result. Calculated details of the SRT are displayed in Fig. 8. The change in EMD takes place in the temperature region between 323 and 331 K, which is at slightly higher temperatures than observed experimentally (Fig. 3). The explanation for this difference is that the calculation is performed for zero field, whereas the experiment has been carried out in a field of 1 T. The calculated temperature dependence of the Ho-sublattice moment is shown in Fig. 9. The interesting feature is that, in the spin-reorientation temperature range, the Ho-sublattice moment decreases slightly in value when the dominant Co-sublattice anisotropy forces the Ho moment away from their easy moment direction. The deviating thermal behavior of the Ho moments in the spin-reorientation temperature range indicates that the Ho moment has the remarkable direction dependence. At high temperature, the easy-axis anisotropy of the Co sublattice dominates the easy-plane anisotropy of the Ho sublattice. The competition between the two opposite anisotropies results in the spin-reorientation transition from an easy b axis to an easy c axis with increasing temperature. The crystal-field calculation shows that the transition is of second order; an easy-cone spin configuration exists in the spin-reorientation temperature range. The Co-sublattice moment increases and the Ho-sublattice moment decreases when they change from a b axis to a c axis. Therefore, when the spin-reorientation transition takes place, the antiparallel arrangement of the Ho- and Co-sublattice moments gives rise to a large step in the thermal curve of the total moment, as shown in Figs. 3 and 7.

A comparison of the calculated (full curves) and experimental (data points) field dependencies of the total moment in the three main directions in the temperature range 100–350 K is presented in Fig. 4. The crystal-field calculation is in good agreement with the experimental result. The saturation magnetization anisotropy can be well reproduced by the crystal-field calculation, both before and after the SRT. Figures 10(a) and 10(b) display the field dependence of the Ho-sublattice moment in $\text{Ho}_2\text{Co}_{15}\text{Si}_2$ at 300 and 350 K, respectively, which is derived from crystal-field calculations for magnetic fields applied along the three major crystallographic directions. At 300 K, the Co- and Ho-sublattice moments are in the b direction at zero field. When the field is applied along the b direction, the Co-sublattice moment will be parallel to the field and the Ho moment antiparallel to the field. Owing to the antiparallel arrangement of the Ho-sublattice moment and the field, an increase of the field will reduce the Ho moment. No difference exists in the field dependence of the Ho moment with the field along the a and b

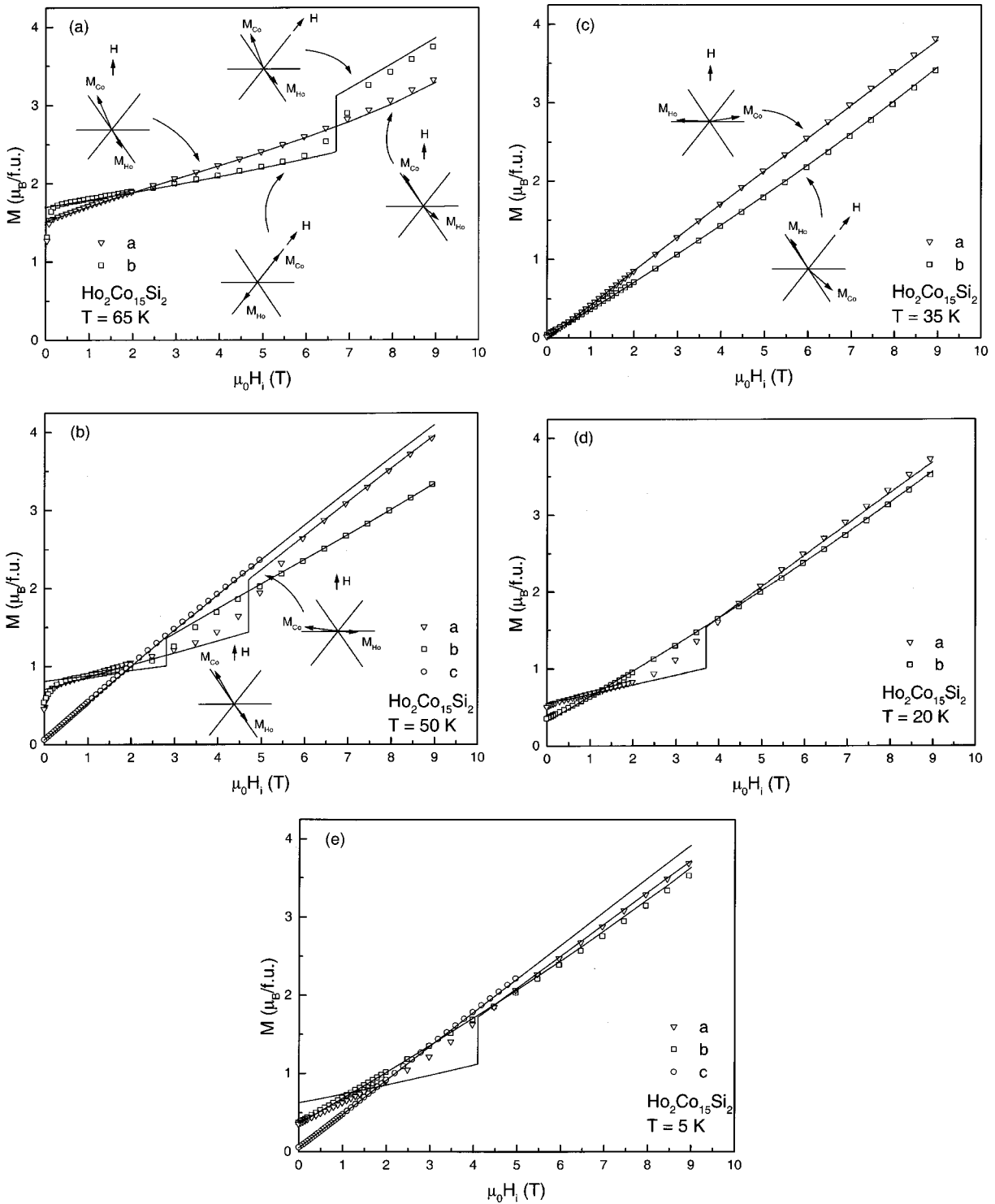


FIG. 11. Field dependence of the total moment in $\text{Ho}_2\text{Co}_{15}\text{Si}_2$ in a temperature range between 65 and 5 K as derived from crystal-field calculations for magnetic fields applied along the crystallographic a , b , and c directions. There is a deviation of 4° from the c direction. Some examples of the moment arrangement in the lowest-energy configuration are shown in diagrams in cases of H parallel to the a or b directions. The six crystallographically equivalent directions shown in the diagrams correspond to the b direction. The experimental data are represented by open symbols.

directions. The reason is that the in-plane anisotropy becomes negligible at high temperatures. When the field is applied along the c direction, below the anisotropy field, an additional strong decrease of the Ho moment occurs, as it is

forced into the c direction. This is due to the strong direction dependence of the Ho moment. The opposite behavior is found above T_{SR} as shown in Fig. 10(b). In zero applied field, all moments are in the c direction and there is some

increase in the Ho moment when it is turned into its easy-plane direction. In the isotherms (Fig. 4) representing the easy direction in particular, one may note a small but steady increase of the total moment with increasing field. Based on the results shown in Figs. 10(a) and 10(b), this appreciable differential susceptibility finds its origin in the reduction of the Ho moments under the influence of the applied field.

We showed already in Figs. 5(a)–5(e) that the low-temperature isotherms are more complicated and give rise to a substantial coercivity upon magnetization reversal. Our model does not include domain-wall dynamics, and hence is unable to describe the coercivity behavior. For this reason, we will only deal with a description of the isotherms in the first quadrant measured with decreasing field. In the calculations we will also disregard any hysteresis accompanying the jump-like transitions observed in some of these isotherms.

A comparison of the experimental and calculated data at temperatures in the interval 65–5 K is made in Figs. 11(a)–11(e). The full curves are the computational results, with symbols representing the experimental data. We have also given examples of the moment arrangement in the lowest-energy configuration corresponding to the various parts of the calculated isotherms. These moment arrangements are represented in diagrams in which the orientation of the Ho- and Co-sublattice moments relative to the six crystallographically equivalent b directions is shown. In Fig. 11(a), it can be seen that the b direction parallel to the field direction is preferred in low fields when the field is applied along the b direction. However, no bending of the Ho and Co moments towards each other occurs in this case, as indicated in the diagram shown at the bottom of the Fig. 11(a). The total moment increases initially more strongly when the field is applied along the a direction, since in this case the possibility of moment bending exists. When the field applied along the b direction becomes sufficiently strong, the moments switch from one b direction to another one, as indicated in the diagram shown at the top of Fig. 11(a). The calculation shows that this switching is accompanied by a sudden jump in the value of the total magnetization. However, the experimental result is a gradual transition, which indicates that domain formation is involved in the switching process. When the applied field is along the a direction, no jump is observed below a field of 9 T at 65 K. In low fields, the Co moment turns into the field direction and the Ho moment turns away from the field direction, as indicated in the left diagram of Fig. 11(a). But in high fields, the Ho moment turns into the field direction and the Co moment turns away from it, as indicated in the right diagram of Fig. 11(a). At 50 K [Fig. 11(b)], a jump takes place in a field of 4.7 T when the field is along the a direction. This jump corresponds to a switching of the moments from the initial b direction to one that is perpendicular to the field, as shown in the diagrams in Fig. 11(b). The jump in the isotherm with the field along the b direction at 50 K has the same origin as that in Fig. 11(a). The jumps in the isotherms with the field along the a direction at 20 and 5 K have the same origin as that in Fig. 11(b). When the field is applied along the c direction at 50 and 5 K, only simple moment bending is observed in Figs. 11(b) and 11(e). No jumps are observed in the isotherms with the field

along both the a and b directions at 35 K in Fig. 11(c). This temperature corresponds to the compensation temperature with zero total moment in zero field. In the presence of an applied field, the lowest-energy configuration is reached for that particular b direction that is perpendicular to the field direction or has an angle of 60° with it. This offers the maximum possibility for moment bending in the basal plane. As shown in the two diagrams in Fig. 11(c), a strictly perpendicular arrangement of the moments with respect to the field can only be reached when the latter is applied along the a direction. This field direction consequently leads to higher values of the total moment than if the field is applied along the b direction. Finally, we wish to discuss the magnetization jumps calculated for the a direction around 4 T in the 20- and 5-K isotherms [Figs. 11(d) and 11(e) respectively]. These field-induced magnetic transitions can be regarded as the origin of the hysteresis observed above the coercivity in Figs. 5(d) and 5(e). Below the compensation temperature, the crystal becomes magnetically harder with decreasing temperature. The complicated domain formation at 5 K makes the crystal-field calculation with the field applied along the a direction deviate seriously from the experimental result when measured in fields lower than the transition field of 4 T.

VI. CONCLUDING REMARKS

We have shown that the magnetic properties of the compound $\text{Ho}_2\text{Co}_{15}\text{Si}_2$ include several interesting phenomena such as field-induced and temperature-induced magnetic phase transitions. Supplementing earlier findings, our results show that the SRT at about 323 K does not proceed directly from easy plane to easy axis but involves a small easy-cone range in between. We also showed that the anisotropy of the saturation magnetization is not exclusively due to the Co sublattice but also originates for a large part from the Ho sublattice. We have been able to reproduce our experimental data in a satisfactory way by means of computational results based on a combination of crystal-field theory and a mean-field two-sublattice model. Through the optimum crystal-field fit, we obtained a set of reliable data relevant to the intrinsic magnetic properties of $\text{Ho}_2\text{Co}_{15}\text{Si}_2$ including CEF parameters, the Ho-Co exchange field, and the Co-sublattice moment. When comparing these values with those reported in the literature for a $\text{Ho}_2\text{Co}_{17}$ single crystal,⁸ one finds that not only the anisotropy of the Co sublattice but also the size of the Co moment and the exchange field are changed by the substitution of Si for Co. As to the CEF parameters, there is hardly any change of the values of A_6^0 and A_6^6 . However, the absolute value of A_2^0 is about 40% larger in $\text{Ho}_2\text{Co}_{15}\text{Si}_2$ than in $\text{Ho}_2\text{Co}_{17}$, while A_4^0 has become much smaller and changed its sign from negative to positive. All these changes give rise to a distinct difference in the intrinsic magnetic properties of $\text{Ho}_2\text{Co}_{17}$ and $\text{Ho}_2\text{Co}_{15}\text{Si}_2$. Furthermore, the large in-plane coercivity at low temperatures and the strong direction dependence of the Ho moment at high temperatures endow the $\text{Ho}_2\text{Co}_{15}\text{Si}_2$ with some interesting and uncommon magnetic phenomena.

ACKNOWLEDGMENTS

The present work was carried out within the scientific exchange program between China and the Netherlands, and

was partly supported by the National Natural Science Foundation of China (Grant No. 59725103) and by the Science and Technology Commission of Shenyang and Liaoning. We would like to thank T. J. Gortenmulder (FOM-ALMOS) for the microprobe analysis.

-
- ¹S. J. Hu, X. Z. Wei, D. C. Zeng, Z. Y. Liu, E. Brück, J. C. P. Klaasse, F. R. de Boer, and K. H. J. Buschow, *Physica B* **270**, 157 (1999).
- ²S. J. Hu, X. Z. Wei, O. Tegus, D. C. Zeng, E. Brück, J. C. P. Klaasse, F. R. de Boer, and K. H. J. Buschow, *J. Alloys Compd.* **284**, 60 (1999).
- ³S. J. Hu, O. Tegus, X. Z. Wei, L. Zhang, D. C. Zeng, Z. Y. Liu, F. R. de Boer, and K. H. J. Buschow, *Acta Phys. Sin.* **49**, 355 (2000).
- ⁴O. Tegus, E. Brück, A. A. Menovsky, F. R. de Boer, and K. H. J. Buschow, *J. Alloys Compd.* **302**, 21 (2000).
- ⁵S. Sinnema, Ph.D. thesis, University of Amsterdam, 1988.
- ⁶M. H. Yu, O. Tegus, Y. Janssen, J. C. P. Klaasse, Z. D. Zhang, E. Brück, F. R. de Boer, and K. H. J. Buschow, *J. Alloys Compd.* **333**, 51 (2002).
- ⁷R. Verhoef, R. J. Radwanski, and Jannu J. M. Franse, *J. Magn. Magn. Mater.* **89**, 176 (1990).
- ⁸X. F. Han, H. M. Jin, Z. J. Wang, T. S. Zhao, and C. C. Sun, *Phys. Rev. B* **47**, 3248 (1993).
- ⁹B. García-Landa, P. A. Algarabel, M. R. Ibarra, F. E. Kayzel, and J. J. M. Franse, *Phys. Rev. B* **55**, 8313 (1997).
- ¹⁰Zhao Tie-song, Jin Han-min, Guo Guang-hua, Han Xiu-feng, and Chen Hong, *Phys. Rev. B* **43**, 8593 (1991).
- ¹¹M. Yamada, H. Kato, H. Yamamoto, and Y. Nakagawa, *Phys. Rev. B* **38**, 620 (1988).
- ¹²F. J. Dyson, *Phys. Rev.* **102**, 1217 (1956); **102**, 1230 (1956).